

# Spin and orbital magnetic moments of molecular beam epitaxy $\gamma'$ -Fe<sub>4</sub>N films on LaAlO<sub>3</sub>(001) and MgO(001) substrates by x-ray magnetic circular dichroism

K. Ito,<sup>1</sup> G. H. Lee,<sup>1</sup> K. Harada,<sup>1</sup> M. Suzuno,<sup>1</sup> T. Suemasu,<sup>1,a)</sup> Y. Takeda,<sup>2</sup> Y. Saitoh,<sup>2</sup> M. Ye,<sup>3</sup> A. Kimura,<sup>3</sup> and H. Akinaga<sup>4</sup>

<sup>1</sup>Institute of Applied Physics, University of Tsukuba, Ibaraki 305-8573, Japan

<sup>2</sup>Japan Atomic Energy Agency, SPring-8, Hyogo 679-5198, Japan

<sup>3</sup>Graduate School of Science, Hiroshima University, Hiroshima 739-8526, Japan

<sup>4</sup>National Institute of Advanced Industrial Science and Technology, Ibaraki 305-8568, Japan

(Received 22 January 2011; accepted 17 February 2011; published online 10 March 2011)

10-nm-thick  $\gamma'$ -Fe<sub>4</sub>N films were grown epitaxially on LaAlO<sub>3</sub>(001) and MgO(001) substrates by molecular beam epitaxy using solid Fe and a radio-frequency NH<sub>3</sub> plasma. The lattice mismatch of these substrates to  $\gamma'$ -Fe<sub>4</sub>N is 0% and 11%, respectively. Spin and orbital magnetic moments of these  $\gamma'$ -Fe<sub>4</sub>N epitaxial films were deduced by x-ray magnetic circular dichroism measurements at 300 K. The total magnetic moments are almost the same for the two substrates, that is,  $2.44 \pm 0.06 \mu_B$  and  $2.47 \pm 0.06 \mu_B$ , respectively. These values are very close to those predicted theoretically, and distinctively larger than that for  $\alpha$ -Fe. © 2011 American Institute of Physics. [doi:10.1063/1.3564887]

Ferromagnetic iron nitrides, such as  $\alpha''$ -Fe<sub>16</sub>N<sub>2</sub>,  $\gamma'$ -Fe<sub>4</sub>N, and  $\epsilon$ -Fe<sub>3</sub>N, are composed of abundant and nontoxic atoms. They have been extensively studied for applications in magnetic devices. In particular, special attention has been paid to chemically and thermally stable  $\gamma'$ -Fe<sub>4</sub>N. The Curie temperature of  $\gamma'$ -Fe<sub>4</sub>N is reported to be 767 K.<sup>1</sup> The electrical conductivities of *up* spins and *down* spins in  $\gamma'$ -Fe<sub>4</sub>N were theoretically calculated by Kokado *et al.*,<sup>2</sup> and according to them, the spin polarization of electrical conductivity [ $P = (\sigma_{\uparrow} - \sigma_{\downarrow}) / (\sigma_{\uparrow} + \sigma_{\downarrow})$ ] at the Fermi level is  $-1$ . Recently, we have confirmed, from point-contact Andreev reflection measurements, that spin polarization in  $\gamma'$ -Fe<sub>4</sub>N thin films grown on MgO(001) substrates by molecular beam epitaxy (MBE) is larger than that in  $\alpha$ -Fe.<sup>3</sup> Furthermore, an inverse tunnel magnetoresistance ratio of  $-75\%$  was reported at room temperature (RT) in CoFeB/MgO/ $\gamma'$ -Fe<sub>4</sub>N magnetic tunnel junctions fabricated by sputtering.<sup>4</sup> Therefore,  $\gamma'$ -Fe<sub>4</sub>N is considered an appropriate material for application in spintronics devices.

$\gamma'$ -Fe<sub>4</sub>N has a cubic perovskite lattice structure, where an N atom is located at the body center of a  $\gamma$ -Fe (fcc structure) unit cell. The lattice constant is 0.3795 nm, which is 1.1 times larger than that of  $\gamma$ -Fe. The unit cell contains two different Fe sites without magnetism, that is, Fe atoms at corner sites and those at face-centered sites. There have been a number of studies on first-principles calculations of magnetic moments at each Fe site in a  $\gamma'$ -Fe<sub>4</sub>N unit cell.<sup>5</sup> According to these, the magnetic moment of an Fe atom at a corner site is approximately  $3.0 \mu_B$ , and that at a face-centered site is approximately  $2.4 \mu_B$ . However, the magnetic moments of  $\gamma'$ -Fe<sub>4</sub>N remain unclear from an experimental point of view. A large magnetic moment of  $2.9 \mu_B$  per Fe atom, was reported for a 55-nm-thick  $\gamma'$ -Fe<sub>4</sub>N thin film grown by sputtering on a lattice-matched LaAlO<sub>3</sub>(LAO)(001) substrate.<sup>6</sup> In this report, the saturation

magnetization per unit volume ( $M_s$ ) was deduced from the magnetic field versus magnetization ( $M$ - $H$ ) curve measured by a vibrating sample magnetometer, where the  $\gamma'$ -Fe<sub>4</sub>N volume was determined from the layer thickness and area. The  $M_s$  values of  $\gamma'$ -Fe<sub>4</sub>N films on SrTiO<sub>3</sub>(STO)(001) and MgO(001) substrates were also evaluated in the same manner. Their lattice mismatches are approximately 3% and 11%, respectively. This implies that the  $M_s$  value in  $\gamma'$ -Fe<sub>4</sub>N increases with decreasing lattice mismatch between  $\gamma'$ -Fe<sub>4</sub>N and a substrate used. However, it is well known that the  $M_s$  value is easily affected by estimation errors when the volume of a  $\gamma'$ -Fe<sub>4</sub>N film is calculated. In addition, the origins of the enhancement in  $M_s$  were not well explained. The purpose of this work was to clarify whether lattice mismatch affects the  $M_s$  value of  $\gamma'$ -Fe<sub>4</sub>N, and also to determine the accurate  $M_s$  value for  $\gamma'$ -Fe<sub>4</sub>N. For this purpose, we prepared high-quality Au(3 nm)/ $\gamma'$ -Fe<sub>4</sub>N(10 nm) epitaxial films by MBE on LAO(001) and MgO(001) substrates. We then deduced the magnetic moments of  $\gamma'$ -Fe<sub>4</sub>N using a superconducting quantum interface device (SQUID) magnetometer and x-ray magnetic circular dichroism (XMCD) measurements. With XMCD, we can obtain the  $M_s$  value of  $\gamma'$ -Fe<sub>4</sub>N free from its volume. There have been several reports on XMCD measurements of  $\gamma'$ -Fe<sub>4</sub>N.<sup>7-10</sup> In Ref. 7, the  $M_s$  value was measured on four-monolayer-thick  $\gamma'$ -Fe<sub>4</sub>N layers on Cu(001), and was reported to be approximately  $2.1 \mu_B$  per Fe atom. However,  $M_s$  values were not systematically evaluated for much thicker  $\gamma'$ -Fe<sub>4</sub>N epitaxial films grown on different substrates such as LAO and STO.

In this letter, Au(3 nm)/ $\gamma'$ -Fe<sub>4</sub>N(10 nm)/LAO(001) (sample A) and Au(3 nm)/ $\gamma'$ -Fe<sub>4</sub>N(10 nm)/MgO(001) (sample B) were grown by MBE using 5N-Fe and rf-NH<sub>3</sub>. After the growth of 10-nm-thick  $\gamma'$ -Fe<sub>4</sub>N layers, 3-nm-thick Au capping layers were subsequently deposited at RT in the same MBE chamber to prevent oxidation of the surfaces. The substrate temperature during the growth was optimized in order to obtain good crystallization and flat surfaces. Substrate temperatures 375 °C and 415 °C were determined to

<sup>a)</sup>Electronic mail: suemasu@bk.tsukuba.ac.jp.

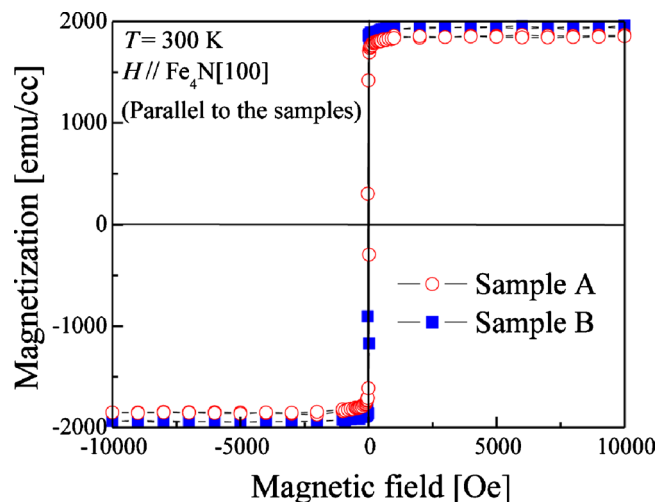


FIG. 1. (Color online)  $M$ - $H$  curves of samples A and B measured by a SQUID magnetometer at 300 K. The external magnetic field applied was parallel to the sample surface.

be suitable for  $\gamma'$ - $\text{Fe}_4\text{N}$  layers on LAO (sample A) and MgO (sample B), respectively. The root-mean-square values of the surface roughness were found to be approximately 0.25 nm for the both samples by atomic force microscopy. The magnetic moments of samples A and B were deduced from SQUID and *ex situ* XMCD measurements at 300 K. For the SQUID measurements, the external magnetic field ( $H$ ) was applied parallel to the sample surface, along the magnetization easy axis. XMCD measurements were performed using the total electron yield method at the BL-23SU beamline of SPring-8 in Japan. Circularly polarized x-rays were incident perpendicular to the sample surface with an external  $H$  of  $\pm 3$  T, applied perpendicular to the sample surface. We confirmed that the magnetic moments of samples A and B were saturated under  $H=3$  T. We also prepared  $\gamma'$ - $\text{Fe}_4\text{N}$  (20 nm) epitaxial layers on  $\text{SrTiO}_3(001)$  (sample C) using MBE at 450 °C. For sample C, the  $H$  dependence of element-specific XMCD intensity was measured for Fe and N atoms at 100 K using the  $\text{Fe } L_3$  (708.0 eV) and N  $K$  (398.8 eV) absorption edges. Circularly polarized x-rays were also incident, perpendicular to the sample surface. The external  $H$  was applied perpendicular to the sample as well. Au capping layers were not deposited on sample C in order to detect the weak signal of the x-ray absorption structure (XAS) related to N atoms. Reflection high-energy electron diffraction and x-ray diffraction patterns showed that the  $\gamma'$ - $\text{Fe}_4\text{N}$  films in samples A–C grew epitaxially, and they were not strained. The details about the crystal growth of samples will be reported elsewhere.

Figure 1 shows the  $M$ - $H$  curves of samples A and B as measured by the SQUID magnetometer at 300 K. Distinct squarelike hysteresis loops with small coercive fields of approximately 20 Oe and large residual magnetization were obtained for both samples. The  $M_s$  values were almost the same for both samples A and B, larger than 1800 emu/cc, corresponding to  $2.65 \mu_B$  per Fe atom; however, the  $M_s$  values are likely to be affected by estimation errors when the volume of the  $\gamma'$ - $\text{Fe}_4\text{N}$  layers was calculated from the layer thickness and the area. Accurate  $M_s$  values of the samples were determined from XMCD measurements, as discussed later.

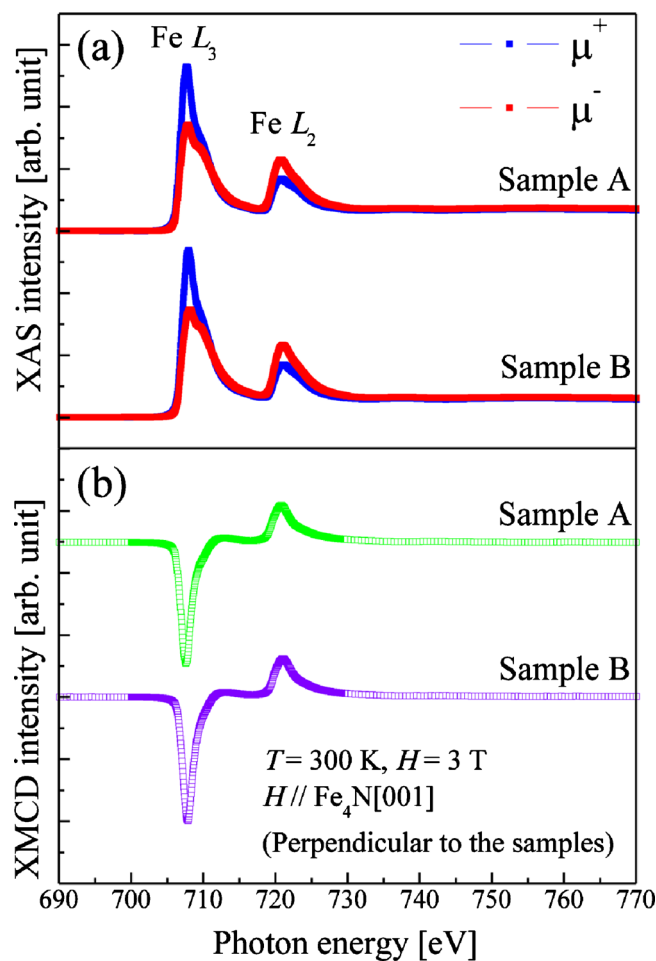


FIG. 2. (Color online) XAS and XMCD spectra of samples A and B observed at 300 K. The external magnetic field ( $H=+3$  T) was perpendicular to the sample surface.

Figure 2 shows (a) XAS and (b) XMCD spectra of samples A and B measured at 300 K under an external  $H$  of +3 T applied perpendicular to the sample surface at 300 K. Distinct MCD spectra were observed at the  $\text{Fe } L_{2,3}$  absorption edge in both samples. MCD spectra measured under the external  $H$  of  $-3$  T were clearly obtained too. The small shoulder structure observed at around 710 eV in the XAS spectrum in Fig. 2(a) has been previously reported,<sup>7,8</sup> and is not caused by surface oxidation layers. We believe that this small shoulder structure is due to splitting of the  $\text{Fe } L_3$  absorption peak caused by different states in three different Fe sites. Spin and orbital magnetic moments of samples A and B were deduced by applying sum-rules analysis.<sup>11–13</sup> The backgrounds of the XAS spectra were removed by subtracting the shrunk integrated XAS spectra from the raw XAS spectra. According to the sum-rules analysis, the magnetic moment is proportional to the hole number of the  $\text{Fe } 3d$  orbit. Thus, an appropriate value should be used in the calculation of magnetic moment. We adopted a value of 3.88 as the hole number of the  $\text{Fe } 3d$  orbit. This value was reported for *in situ* XMCD measurement of  $\gamma'$ - $\text{Fe}_4\text{N}/\text{Cu}(001)$ .<sup>7</sup> The spin, orbital, and total magnetic moments of samples A and B are summarized in Table I. The reported values of the magnetic moments of  $\gamma'$ - $\text{Fe}_4\text{N}$ ,  $\epsilon$ - $\text{Fe}_3\text{N}$ , and  $\alpha$ -Fe are also shown for comparison.<sup>5,13,14</sup> The total magnetic moments of  $\gamma'$ - $\text{Fe}_4\text{N}$  in samples A and B were calculated to be  $2.44 \pm 0.06 \mu_B$  and  $2.47 \pm 0.06 \mu_B$  per Fe atom, respectively, corresponding to

TABLE I. Spin and orbital magnetic moments of iron nitrides and  $\alpha$ -Fe deduced by experimental and theoretical analyses.

Compounds	Magnetic moment ( $\mu_B$ per Fe atom)			Method	Reference
	$m_{orb}$	$m_{spin}$	$m_{total}$		
$\gamma'$ -Fe <sub>4</sub> N/LAO	$0.102 \pm 0.003$	$2.34 \pm 0.06$	$2.44 \pm 0.06$	Experiment	This work
$\gamma'$ -Fe <sub>4</sub> N/MgO	$0.121 \pm 0.003$	$2.35 \pm 0.06$	$2.47 \pm 0.06$	Experiment	This work
$\gamma'$ -Fe <sub>4</sub> N	0.068	2.52	2.59	Theory	5
$\epsilon$ -Fe <sub>3</sub> N	0.040	1.97	2.01	Theory	14
$\alpha$ -Fe	0.086	1.98	2.07	Experiment	13
$\alpha$ -Fe	0.046	2.16	2.21	Theory	14

$M_s = 1680$  emu/cc. These are almost the same, and are much closer to the theoretically predicted value of  $2.59 \mu_B$  (Ref. 5) than that experimentally obtained from the  $M$ - $H$  curves ( $2.9 \mu_B$ ).<sup>6</sup> We think that our result is more reliable than that measured on the four-monolayer-thick  $\gamma'$ -Fe<sub>4</sub>N layers.<sup>7</sup> We compared our result with a theoretical value of  $2.59 \mu_B$ , obtained by the Perdew–Burke–Ernzerhof functional plus Hubbard  $U$  ( $U=0.4$  eV) (PBE+ $U$ ) method,<sup>5</sup> because they insisted that the PBE+ $U$  method is the best currently available for structural properties of  $\gamma'$ -Fe<sub>4</sub>N as well as its magnetic properties. Here, the  $M_s$  value is calculated to be  $[(2.92 + 0.06) + (2.39 + 0.06) \times 2 + (2.39 + 0.09)]/4 = 2.59 \mu_B$  per Fe atom from the values listed in Table 10 of Ref. 5. On the basis of these results, we conclude that the  $M_s$  value in  $\gamma'$ -Fe<sub>4</sub>N does not change depending on lattice mismatch between  $\gamma'$ -Fe<sub>4</sub>N and the substrate used as long as  $\gamma'$ -Fe<sub>4</sub>N is not strained. We should also note that the  $M_s$  value of  $\gamma'$ -Fe<sub>4</sub>N is significantly larger than that of  $\epsilon$ -Fe<sub>3</sub>N and  $\alpha$ -Fe.

Figure 3 shows the  $H$  dependence of element-specific XMCD signals for Fe and N atoms in sample C measured at 100 K. Incident photon energies of the x-rays were set to 708.0 eV and 398.8 eV, which correspond to the Fe  $L_3$  and N  $K$  absorption peak energies, respectively. We could clearly find that the XMCD intensity for N atoms follows that for the Fe atoms, meaning that the magnetic moment is induced at the N sites probably by band hybridization between the  $3d$  orbit of Fe and the  $2p$  orbit of N. Thus, spins of Fe and N

atoms are coupled to the ferromagnetic configuration.

In summary, spin and orbital magnetic moments of  $\gamma'$ -Fe<sub>4</sub>N(10 nm) epitaxial films on LAO(001) and MgO(001) substrates by MBE were deduced by XMCD measurements. The total magnetic moments using an Fe  $3d$  hole number of 3.88 were deduced to be  $2.44 \pm 0.06 \mu_B$  and  $2.47 \pm 0.06 \mu_B$ , respectively. It can at least be stated that the  $M_s$  value in  $\gamma'$ -Fe<sub>4</sub>N does not change depending on lattice mismatch between  $\gamma'$ -Fe<sub>4</sub>N and the substrate used, and that the  $M_s$  is clearly larger than that of  $\epsilon$ -Fe<sub>3</sub>N and  $\alpha$ -Fe. The element-specific  $H$  dependence of XMCD intensity curves for a 20-nm-thick  $\gamma'$ -Fe<sub>4</sub>N epitaxial film on a STO(001) substrate showed that the MCD intensity for an N atom followed that for an Fe atom, showing that magnetic moments are probably induced in the N sites by band hybridization between Fe and N atoms.

This work was supported in part by a Grant-in-Aid for Scientific Research on Priority Area of “Creation and Control of Spin Current” (Grant No. 19048029) from the MEXT of Japan, and by the NanoProcessing Partnership Platform (NPPP) at AIST, Tsukuba. XMCD measurements were performed at JAEA SPring-8 BL-23SU under Nanonet Support Proposals (Grant Nos. 2010A3877 and 2010B1738).

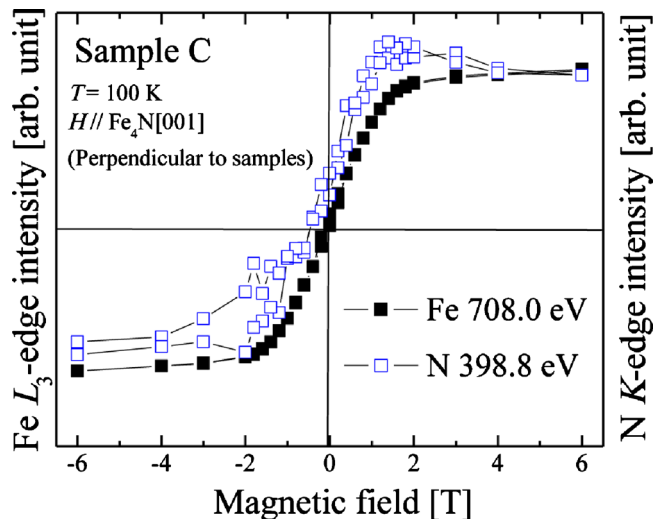


FIG. 3. (Color online)  $H$  dependence of element-specific XMCD intensities for Fe and N atoms in sample C measured at 100 K. The external magnetic field was applied perpendicular to the sample surface.

<sup>1</sup>G. Shirane, W. J. Takei, and S. L. Ruby, *Phys. Rev.* **126**, 49 (1962).

<sup>2</sup>S. Kokado, N. Fujima, K. Harigaya, H. Shimizu, and A. Sakuma, *Phys. Rev. B* **73**, 172410 (2006).

<sup>3</sup>A. Narahara, K. Ito, T. Suemasu, Y. K. Takahashi, A. Rajanikanth, and K. Hono, *Appl. Phys. Lett.* **94**, 202502 (2009).

<sup>4</sup>Y. Komasaki, M. Tsunoda, S. Isogami, and M. Takahashi, *J. Appl. Phys.* **105**, 07C928 (2009).

<sup>5</sup>See, for example, E. L. P. Blanca, J. Desimoni, N. E. Christensen, H. Emmerich, and S. Cottenier, *Phys. Status Solidi B* **246**, 909 (2009).

<sup>6</sup>S. Atiq, H. S. Ko, S. A. Siddiqi, and S. C. Shin, *Appl. Phys. Lett.* **92**, 222507 (2008).

<sup>7</sup>Y. Takagi, K. Isami, I. Yamamoto, T. Nakagawa, and T. Yokoyama, *Phys. Rev. B* **81**, 035422 (2010).

<sup>8</sup>C. S. Hanke, R. G. Arrabal, J. E. Prieto, E. Andrzejewska, N. Gordillo, D. O. Boerma, R. Loloee, J. Skuza, and R. A. Lukaszew, *J. Appl. Phys.* **99**, 08B709 (2006).

<sup>9</sup>N. D. Telling, G. van der Laan, M. T. Georgieva, and N. R. S. Farley, *Rev. Sci. Instrum.* **77**, 073903 (2006).

<sup>10</sup>N. Ishimatsu, H. Maruyama, N. Kawamura, M. Suzuki, Y. Ohishi, M. Ito, S. Nasu, T. Kawakami, and O. Shimomura, *J. Phys. Soc. Jpn.* **72**, 2372 (2003).

<sup>11</sup>B. T. Thole, P. Carra, F. Sette, and G. van der Laan, *Phys. Rev. Lett.* **68**, 1943 (1992).

<sup>12</sup>P. Carra, B. T. Thole, M. Altarelli, and X. D. Wang, *Phys. Rev. Lett.* **70**, 694 (1993).

<sup>13</sup>C. T. Chen, Y. U. Idzerda, H. J. Lin, N. V. Smith, G. Meigs, E. Chaban, G. H. Ho, E. Pellegrin, and F. Sette, *Phys. Rev. Lett.* **75**, 152 (1995).

<sup>14</sup>M. Alouani, J. M. Wills, and J. W. Wilkins, *Phys. Rev. B* **57**, 9502 (1998).